THE JOURNAL OF PHYSICAL CHEMISTRY Letters

Letter

pubs.acs.org/JPCL

Fundamental Bulk/Surface Structure–Photoactivity Relationships of Supported $(Rh_{2-y}Cr_yO_3)$/GaN Photocatalysts

Somphonh P. Phivilay,[†] Charles A. Roberts,[†,⊥] Alexander A. Puretzky,[‡] Kazunari Domen,[§] and Israel E. Wachs*[,†]

[†]Operando Molecular Spectroscopy & Catalysis Laboratory, Department of Chemical Engineering, Lehigh University, Bethlehem, Pennsylvania 18015, United States

[‡]Center for Nanophase Materials Sciences and Materials Science and Technology Division, Oak Ridge National Laboratory, Oak Ridge, Tennessee 37831, United States

[§]Department of Chemical System Engineering, University of Tokyo, 7-3-1 Hongo, Bunkyo-ku, Tokyo 113-8656, Japan

Supporting Information

ABSTRACT: The supported $(Rh_{2-y}Cr_yO_3)$/GaN photocatalyst was examined as a model nitride photocatalyst system to assist in the development of fundamental structure–photoactivity relationships for UV activated water splitting. Surface characterization of the outermost surface layers by high-sensitivity low energy ion scattering (HS-LEIS) and high-resolution X-ray photoelectron spectroscopy (HR-XPS) revealed that the GaN support consists of a GaO_x outermost surface layer on a thin film of GaO_xN_y. HR-XPS demonstrates that the supported $(Rh_{2-y}Cr_yO_3)$ mixed oxide nanoparticles (NPs) consist of Cr^{3+} and Rh^{3+} cations that are surface enriched for $(Rh_{2-y}Cr_yO_3)$/GaN. Raman and UV–vis spectroscopy show that the bulk molecular and electronic structures, respectively, of the GaN support are not perturbed by the deposition of the $(Rh_{2-y}Cr_yO_3)$ NPs. The function of the GaN bulk lattice is to generate photoexcited electrons/holes, with the electrons harnessed by the surface Rh^{3+} sites for evolution of H_2 and the holes trapped at the Ga oxide/oxynitride surface sites for splitting of water and evolving O_2.

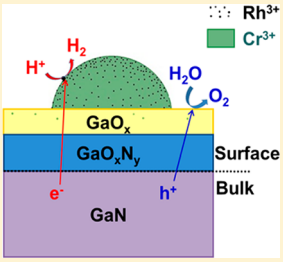

SECTION: Surfaces, Interfaces, Porous Materials, and Catalysis

Early research on photocatalytic water splitting primarily focused on the use of semiconductor metal oxide materials with UV irradiation.[1−3] More recently, nonoxide materials have been discovered that are also able to perform photocatalytic water splitting with visible excitation.[4] Unlike the extensive list (>130) of metal oxide semiconductors that can perform photocatalytic water splitting, only a handful of bulk oxynitride materials with d^{10} electronic configuration that are active for overall photocatalytic water splitting have been discovered: Ge_3N_4,[5−8] $(Ga_{1-x}Zn_x)(N_{1-x}O_x)$,[9−13] $(Zn_{1+x}Ge)(N_2O_x)$,[14] and GaN.[15−17] Other bulk oxynitride materials have also been discovered with d^0 electronic configurations (Ti, Ta, and Nb) that are able to produce H_2 and O_2 with sacrificial reagents, but only modified TaON is capable of photocatalytic water splitting in pure water.[2,4,18] The limited number of bulk oxynitride photocatalysts discovered so far that are capable of water splitting suggests that water splitting is a greater challenge for oxynitrides compared to metal oxide photocatalysts. Although other mixed metal oxynitride materials are more active than GaN and can utilize visible light for photocatalytic water splitting, it is important to develop fundamental structure/photoactivity relationships for this basic nitride photocatalyst because it is a component of $(Ga_{1-x}Zn_x)(N_{1-x}O_x)$ oxynitride photocatalysts. Furthermore, understanding how the GaN photocatalyst functions can be important for the design of advanced oxynitride photocatalysts.

The present study focuses on the bulk GaN semiconductor photocatalyst. Although GaN has been found to be unable to photocatalytically split water, it becomes part of an active photocatalyst material with UV excitation (λ > 300 nm) when $(Rh_{2-y}Cr_yO_3)$ mixed oxide nanoparticles (NPs) are deposited on its surface (photonic efficiency (P.E.) of 0.7%).[17] The present investigation will apply surface and bulk characterization methods to obtain fundamental insights about this photocatalyst system. Information about the outermost surface layer (∼0.3 nm) and surface region (∼1–3 nm) of the supported $(Rh_{2-y}Cr_yO_3)$/GaN photocatalyst system will be accessed with high-sensitivity low energy ion scattering (HS-LEIS) spectroscopy and high-resolution X-ray photoelectron spectroscopy (HR-XPS), respectively. Insights into the bulk molecular and electronic structures of the GaN phase and influence of the supported $(Rh_{2-y}Cr_yO_3)$ NPs upon the GaN phase properties will be obtained with in situ optical spectroscopic characterization (Raman, UV–vis, and photoluminescence (PL)).

The Raman spectra for the GaN photocatalysts are presented in Figure 1 and exhibit characteristic bands associated with the phonon modes of the hexagonal wurtzite GaN crystal

Received: September 3, 2013
Accepted: October 15, 2013

   dx.doi.org/10.1021/jz401884c | J. Phys. Chem. Lett. 2013, 4, 3719−3724

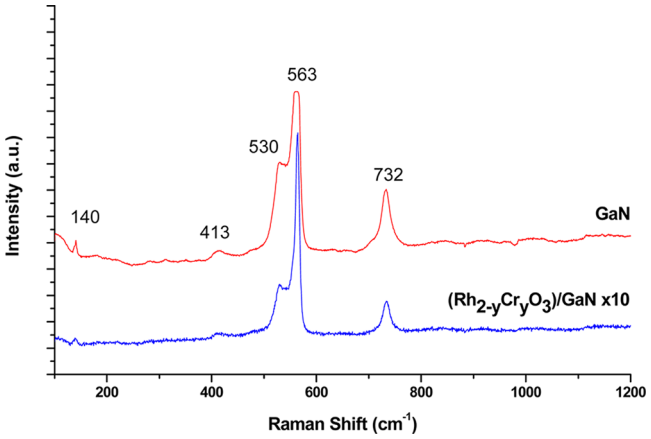

Figure 1. Raman spectra of GaN and supported $(Rh_{2-y}Cr_yO_3)$/GaN photocatalysts (532 nm) under ambient conditions.

structure.[19,20] The Raman band at 140 cm^{-1} has been assigned to the E_2 phonon mode, the 413 cm^{-1} band is a combination of optical and acoustic modes, the 530 and 563 cm^{-1} bands are the transverse optical (TO) modes of A_1 and E_1, respectively, and the 732 cm^{-1} band is from the combination of the longitudinal optical modes of A_1 and E_1.[19,20] The Raman spectrum of the supported $(Rh_{2-y}Cr_yO_3)$/GaN photocatalyst is still dominated by the GaN vibrations, but is much weaker than that of pure GaN because of the darker sample color resulting from the deposition of $(Rh_{2-y}Cr_yO_3)$ mixed oxides. The Raman bands of crystalline Cr_2O_3 (542 and 603 cm^{-1})[21,22] and crystalline Rh_2O_3 (550 cm^{-1})[23] are not detectable because of the strong GaN Raman bands in the 500−600 cm^{-1} region. The Raman bands for $(Rh_{2-y}Cr_yO_3)$ mixed oxide are also expected in the same vibrational range. Importantly, the Raman spectra demonstrate that the bulk molecular structure of the GaN phase is unperturbed by deposition of the $(Rh_{2-y}Cr_yO_3)$ mixed oxide NPs.

The UV−vis diffuse reflectance spectroscopy (DRS) optical band gap (Eg) values for the bulk GaN and $(Rh_{2-y}Cr_yO_3)$/GaN are ∼3.3 eV, indicating that the optical band gap of bulk GaN is essentially unperturbed by the deposition of the $(Rh_{2-y}Cr_yO_3)$ mixed oxide NPs. This indicates that the bulk GaN component dominates the UV−vis absorbance spectrum of the supported $(Rh_{2-y}Cr_yO_3)$/GaN photocatalyst system.

The atomic compositions of GaN and $(Rh_{2-y}Cr_yO_3)$/GaN in the surface region (∼1−3 nm) were measured with ex situ HR-XPS and given in Table 1. The surface region for the bulk

Table 1. HR-XPS Atomic Composition of Surface Region (∼1−3 nm) of GaN Photocatalysts

element	GaN	$(Rh_{2-y}Cr_yO_3)$/GaN
O 1s	19.0%	39.5%
N 1s	62.0%	41.1%
Ga 2p 3/2	19.0%	9.5%
Cr 2p 3/2	0.0%	6.7%
Rh 3d	0.0%	3.2%

GaN consists only of Ga, N, and O, and no other elements were detected. Note that the O/Ga∼1 atomic ratio in the surface region indicates that Ga is extensively oxidized in the surface region from exposure to ambient conditions. As expected for deposition of an oxide on GaN and its short calcination in air at 623 K (see Experimental Methods section below for synthesis conditions), the addition of the $(Rh_{2-y}Cr_yO_3)$ mixed oxide NPs to the GaN support doubles the O concentration, while decreasing the concentration of the GaN support elements (by ∼50% Ga and ∼30% N). The surface concentration of Rh and Cr are ∼3× and ∼4.5× greater than their bulk concentrations, consistent with the deposition of Rh and Cr on the on the surface of the GaN support.

The HR-XPS *ex situ* surface analysis also contains information on the chemical state of Cr and Rh in the supported $(Rh_{2-y}Cr_yO_3)$/GaN photocatalyst and is presented in Figure 2.

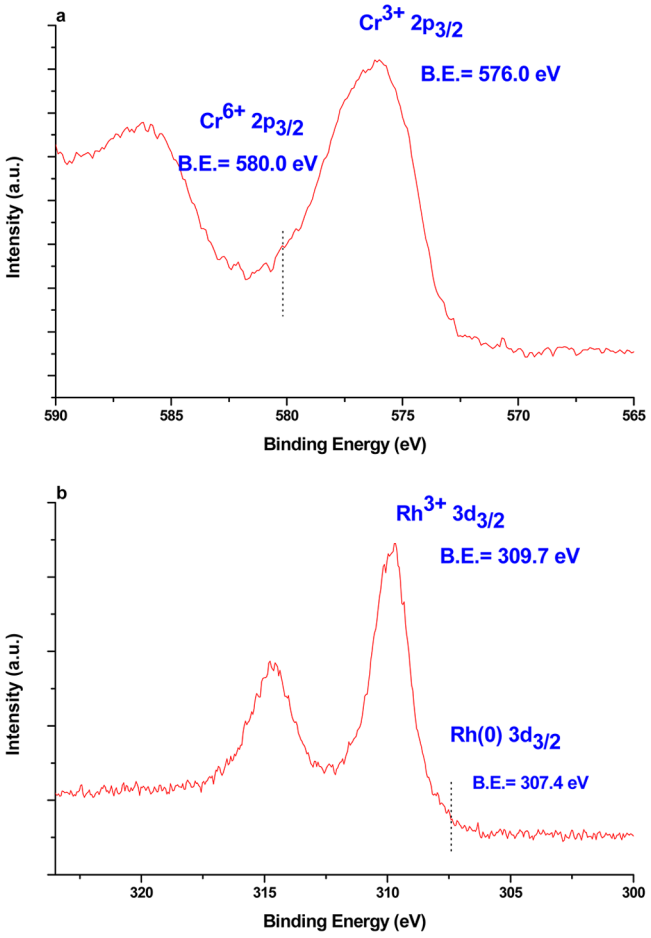

Figure 2. HR-XPS spectra of (a) Cr 2p and (b) Rh 3d regions of the supported $(Rh_{2-y}Cr_yO_3)$/GaN photocatalyst.

The HR-XPS spectra for the Cr 2p and Rh 3d regions of the supported $(Rh_{2-y}Cr_yO_3)$/GaN photocatalyst reveal the presence of only Cr^{3+} and Rh^{3+} and the absence of Cr^{6+} or metallic Rh(0) in the surface region, as expected from the air calcination treatment at 623 K.

The outermost surface layer (∼0.3 nm) and the layers immediately below the surface of bulk GaN were analyzed with dynamic HS-LEIS employing a He^+ ion gas source, and the findings are shown in Figure 3. The HS-LEIS signal for N is almost absent from the topmost surface layer and significantly increases in intensity into a definable peak with further sputtering into the layers below the outermost surface layer. Although Ga is present on the topmost surface layer, its HS-LEIS signal also significantly increases with depth profiling. In contrast to that of Ga and N, the HS-LEIS signal for O is strongest on the outermost layer and decreases with sputtering into the bulk demonstrating surface enrichment of O from

dx.doi.org/10.1021/jz401884c | J. Phys. Chem. Lett. 2013, 4, 3719−3724

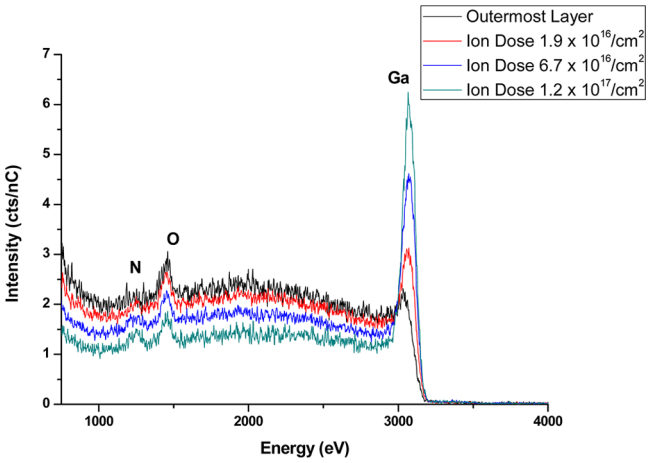

Figure 3. HS-LEIS depth profile for untreated GaN photocatalyst using He^+ ion gas.

exposure to ambient conditions. The HS-LEIS sputtering findings reveal that the outermost surface layer of GaN consists of GaO_x and that a thin Ga oxynitride (GaO_xN_y) film is present in the layers below the topmost surface layer.

The HS-LEIS spectra comparing the untreated and atomic oxygen pretreated supported ($Rh_{2-y}Cr_yO_3$)/GaN photocatalyst are presented in Figure 4. The oxidation pretreatment method

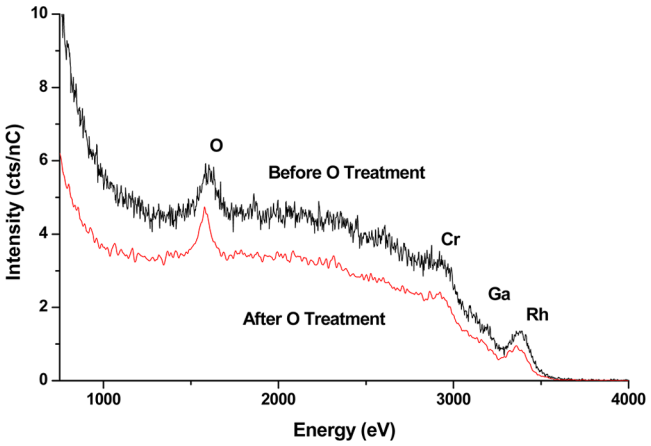

Figure 4. HS-LEIS spectra of untreated and atomic O treated supported ($Rh_{2-y}Cr_yO_3$)/GaN photocatalyst with He^+ ion gas.

(see Supporting Information) was used to clean off hydrocarbon deposits on the outermost surface, increase the signal intensity, and was not found to affect the outermost surface composition of the photocatalyst. The HS-LEIS depth profiles for the supported ($Rh_{2-y}Cr_yO_3$)/GaN photocatalyst pretreated with atomic O are presented in Figure 5. From the He^+ ions gas HS-LEIS measurement (Figure 5a), the outermost surface layer contains O, Cr, Ga, and Rh and does not contain any detectable N. It appears that the oxidation treatment to form the supported ($Rh_{2-y}Cr_yO_3$) mixed oxide NPs on the GaN support also oxidized the outer surface layers of GaN and is consistent with the 100% increase of the XPS O concentration in the surface region (see Table 1).[24]

More quantitative depth profiling information is provided with Ne^+ depth profiling HS-LEIS analysis as shown in Figure 5b. The increased sensitivity of Ne^+ ions for heavy metals revealed the presence of trace amounts of Sn and Ba in the outermost

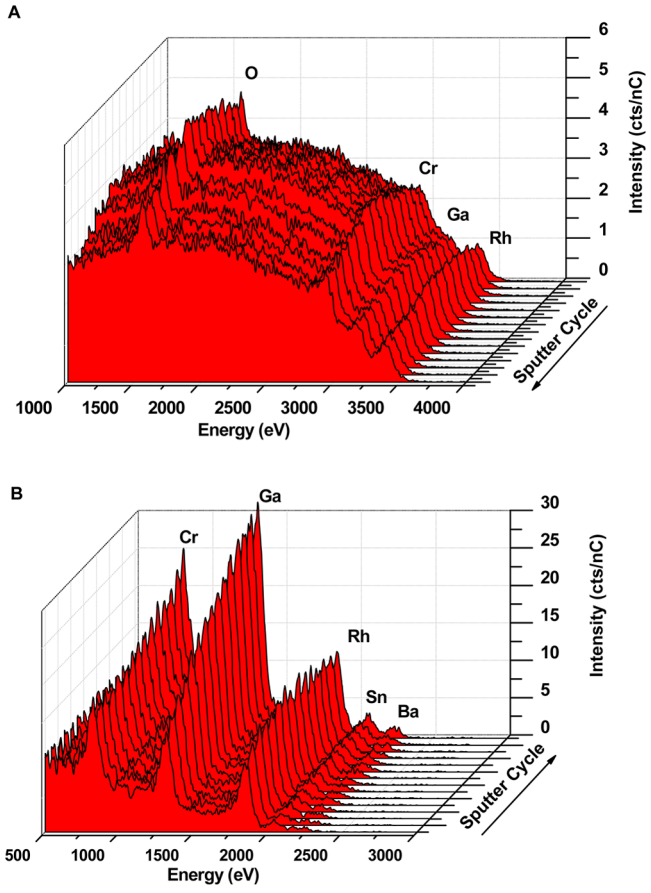

Figure 5. HS-LEIS depth profile for the supported ($Rh_{2-y}Cr_yO_3$)/GaN photocatalyst after atomic O pretreatment using (a) He^+ ion gas and (b) Ne^+ ion gas.

surface layers, which may have come from handling of the material during and after impregnation of the $Cr(NO_3)_3{\cdot}9H_2O$ and $Na_3RhCl_6{\cdot}2H_2O$ precursors since bulk GaN did not exhibit these trace impurities. The HS-LEIS signals for Cr and Rh were quantified against metallic Cr and Rh standards (surface density ~1 × 10^{15} atoms/cm^2) and their quantitative depth profile atomic concentrations are presented in Figure 6. The

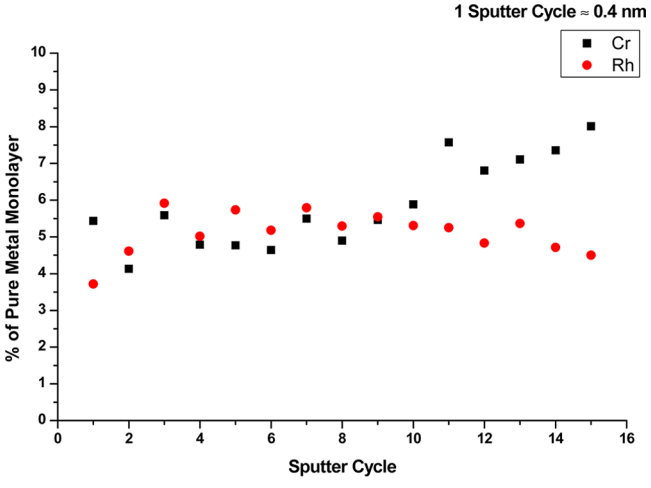

Figure 6. HS-LEIS depth profile of Cr and Rh for supported ($Rh_{2-y}Cr_yO_3$)/GaN photocatalyst using Ne^+ ion gas after O pretreatment.

dx.doi.org/10.1021/jz401884c | J. Phys. Chem. Lett. 2013, 4, 3719−3724

outermost surface layer contains a higher concentration of Cr, ~5.4%, than Rh, ~3.7%, while the layers below the outermost surface show that the concentration of Cr and Rh are relatively comparable at ~4.5−5.5%. The concentration of Cr becomes larger than Rh again at deeper layers below the surface. The increase in the concentration of Cr at deeper layers may be indicative of greater Cr concentration in the deeper layers of the $(Rh_{2-y}Cr_yO_3)$ NPs and possibly the presence of dissolved Cr beneath the surface. The concentrations of Rh and Cr are significantly enriched at all depths of the surface region compared to their bulk concentrations (0.8% Rh and 0.3% Cr).

The population of electron/hole recombination centers in a photocatalyst is reflected in the intensity of the PL emissions spectra.[25,26] The steady-state PL emissions spectra with 400 nm excitation for the GaN and supported $(Rh_{2-y}Cr_yO_3)$/GaN photocatalysts exhibit broad emission maxima at 725 and 710 nm, respectively, as shown in Figure 7. Deposition of the

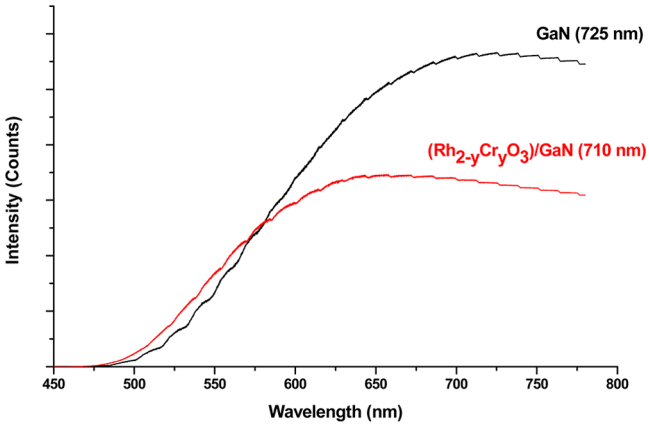

Figure 7. PL emissions spectra for GaN photocatalysts (400 nm excitation).

$(Rh_{2-y}Cr_yO_3)$ mixed oxide NPs on the GaN support diminishes the intensity of the PL emission indicating that the photoexcited electrons are being trapped by the supported $(Rh_{2-y}Cr_yO_3)$ NPs at the mixed oxide/GaN interface and, therefore, are unavailable for recombining with holes in the GaN bulk lattice. In other words, the supported $(Rh_{2-y}Cr_yO_3)$ NPs on the GaN support act as efficient electron traps for the photoexcited electrons generated from the GaN bulk and, consequently, minimize electron/hole recombination and promote charge transfer to the surface.[26−28]

The PL peak position is directly related to the band gap of a material, however, UV−vis spectroscopy detected no change in the band gap when comparing GaN to $(Rh_{2-y}Cr_yO_3)$/GaN (3.3 eV). Thus, it appears that PL spectroscopy is more sensitive to the changes in the band gap energy. Indeed, the blue shift in PL from 725 to 710 nm is only a 0.04 eV difference (1.71 to 1.75 eV). A blue shift in the PL peak often corresponds to a shift to lower dimensional semiconductors.[29] The current results indicate that the addition of $(Rh_{2-y}Cr_yO_3)$ to the GaN induces a lower dimensional semiconductor surface layer at the mixed oxide/GaN interface, which is detected in the PL spectra as the observed 15 nm blue shift. The presence of lower dimensional semiconductor trap states at surface $(Rh_{2-y}Cr_yO_3)$/GaN sites is predicted to be beneficial to the photoactivity as electrons trapped at these sites are longer lived (lower PL intensity), higher energy, and closely associated with the surface, which are all factors that are expected to improve photoactivity.

The above surface and bulk characterization studies reveal that the supported $(Rh_{2-y}Cr_yO_3)$/GaN photocatalyst is a multiphasic system with $(Rh_{2-y}Cr_yO_3)$ NPs, consisting of Rh^{3+} and Cr^{3+} cations, supported on the GaN substrate. The current surface characterization studies show for the first time that the GaN support consists of a GaN bulk lattice with a thin GaO_xN_y film (~1−3 nm) that is capped by a GaO_x outermost surface layer. Some Cr^{3+} and Rh^{3+} cations may also be incorporated in the thin GaO_xN_y oxynitride outermost layers.

The GaN photocatalysts are compared with the $(Ga_{1-x}Zn_x)$-$(N_{1-x}O_x)$ photocatalysts because both materials consist of a oxynitride thin film in the surface region. The photoactivity mass normalized turnover rates (TOR_m) of GaN, $(Rh_{2-y}Cr_yO_3)$/GaN, $(Ga_{1-x}Zn_x)(N_{1-x}O_x)$, $Rh_2O_3/(Ga_{1-x}Zn_x)(N_{1-x}O_x)$, $Cr_2O_3/(Ga_{1-x}Zn_x)(N_{1-x}O_x)$ and $(Rh_{2-y}Cr_yO_3)/(Ga_{1-x}Zn_x)$-$(N_{1-x}O_x)$ are given in Table 2. The $(Ga_{1-x}Zn_x)(N_{1-x}O_x)$ oxynitride and supported $Cr_2O_3/(Ga_{1-x}Zn_x)(N_{1-x}O_x)$ materials are unable to photocatalytically split water while supported $Rh_2O_3/(Ga_{1-x}Zn_x)(N_{1-x}O_x)$ is able to nonstoichiometrically form H_2:O_2 (50:1).[10,30] The supported $(Rh_{2-y}Cr_yO_3)/(Ga_{1-x}Zn_x)(N_{1-x}O_x)$ photocatalyst, however, increases the TOR_m for splitting of water by 77× and yields stoichiometric amounts of H_2 and O_2. Similarly for the GaN photocatalysts with the thin oxynitride surface film, GaN is not active for splitting of water and only when the $(Rh_{2-y}Cr_yO_3)$ mixed oxide NPs are deposited on the GaN support does this photocatalyst system yield significant amounts of stoichiometric H_2 and O_2.[17] It has been proposed that the addition of Cr^{3+} facilitates charge transfer from the bulk $(Ga_{1-x}Zn_x)(N_{1-x}O_x)$ to the $Rh_{2-y}Cr_yO_3$ NPs and that it could help to promote the creation of photoactive sites on $Rh_{2-y}Cr_yO_3$ NPs.[31] The same mechanism could also be responsible for activating the $(Rh_{2-y}Cr_yO_3)$/GaN photocatalyst. The water splitting performance of the $(Ga_{1-x}Zn_x)(N_{1-x}O_x)$− and GaN-based photocatalysts demonstrate the critical role of Rh^{3+} cations in the $(Rh_{2-y}Cr_yO_3)$ NPs for photocatalytic splitting of H_2O.

Table 2. Photoactivity of GaN and $(Ga_{1-x}Zn_x)(N_{1-x}O_x)$ Photocatalysts

photocatalyst	BET [m^2/g]	TOR_m[a] [H_2 μmol/g/h]	TOR_s[b] [H_2 μmol/m/h]	N_s [Rh sites/g]	TOF [1/s]
GaN	0.3	0	0	-	-
$(Rh_{2-y}Cr_yO_3)$/GaN	0.3	6.3×10^1	2.1×10^2	1.1×10^{17}	9.5×10^{-2}
$(Ga_{1-x}Zn_x)(N_{1-x}O_x)$	7.4	0	0	-	-
$(Rh_2O_3)/(Ga_{1-x}Zn_x)(N_{1-x}O_x)$	7.4	1.7×10^2	2.3×10^1	-	-
$(Cr_2O_3)/(Ga_{1-x}Zn_x)(N_{1-x}O_x)$	7.4	0	0	-	-
$(Rh_{2-y}Cr_yO_3)/(Ga_{1-x}Zn_x)(N_{1-x}O_x)$	7.4	1.3×10^4	1.7×10^3	9.5×10^{17}	2.2×10^0

Excitation source: 450 W high-pressure Hg lamp (λ > 300 nm); 0.3g photocatalyst used. Photoactivity data (TOR_m and TOR_s) obtained from refs 17 and 30. [a]TOR_m: mass normalized turnover rate. [b]TOR_s: surface normalized turnover rate.

dx.doi.org/10.1021/jz401884c | J. Phys. Chem. Lett. 2013, 4, 3719−3724

The photoactivity turnover rates were also surface area normalized (TOR_s) in Table 2 to allow for better comparison between the different photocatalysts given the 25× larger surface area of $(Ga_{1-x}Zn_x)(N_{1-x}O_x)$ relative to GaN. As already indicated, only in the presence of $(Rh_{2-y}Cr_yO_3)$ NPs are stoichiometric amounts of H_2 and O_2 produced. The TOR_s photoactivity for H_2 production by supported $(Rh_{2-y}Cr_yO_3)$/GaN is an order of magnitude greater that of supported Rh_2O_3/$(Ga_{1-x}Zn_x)(N_{1-x}O_x)$ and that by supported $(Rh_{2-y}Cr_yO_3)$/$(Ga_{1-x}Zn_x)(N_{1-x}O_x)$ is another order of magnitude greater than that by supported $(Rh_{2-y}Cr_yO_3)$/GaN. The enhanced photocatalytic performance of supported $(Rh_{2-y}Cr_yO_3)$/$(Ga_{1-x}Zn_x)(N_{1-x}O_x)$ compared to $(Rh_{2-y}Cr_yO_3)$/GaN is related to the greater photon absorption by supported $(Rh_{2-y}Cr_yO_3)$/$(Ga_{1-x}Zn_x)(N_{1-x}O_x)$ that is reflected in its lower optical band gap (2.6 vs 3.3 eV) or optimized photonic efficiency (5.9 vs 0.7%) and, thus, a much greater number of photoexcited electrons and holes are produced in the bulk lattice of $(Ga_{1-x}Zn_x)(N_{1-x}O_x)$ than GaN. The lower optical band gap of the $(Ga_{1-x}Zn_x)(N_{1-x}O_x)$ compared to GaN has been ascribed to differences in the valence band orbitals where only N2p orbitals exist in the GaN while N2p, Zn3d, and O2p orbitals exist for the $(Ga_{1-x}Zn_x)(N_{1-x}O_x)$. The p−d repulsion between N2p and Zn3d orbitals in the valence band of the $(Ga_{1-x}Zn_x)(N_{1-x}O_x)$ has been theorized as the reason for the lower band gap energy of the $(Ga_{1-x}Zn_x)(N_{1-x}O_x)$.[32]

The number of surface Rh^{3+} sites per gram photocatalyst (N_s) on the outermost surface layer, the first spectrum of HS-LEIS depth profile, allowed calculation of turnover frequency (TOF: number of H_2 molecules produced per exposed Rh^{3+} site per second) for the supported $(Rh_{2-y}Cr_yO_3)$/GaN and $(Rh_{2-y}Cr_yO_3)$/$(Ga_{1-x}Zn_x)(N_{1-x}O_x)$ and are also given in Table 2. Both photocatalysts contain 1 wt % Rh, however, the supported $(Rh_{2-y}Cr_yO_3)$/$(Ga_{1-x}Zn_x)(N_{1-x}O_x)$ photocatalyst has a greater number of exposed surface Rh^{3+} sites per gram photocatalyst than the supported $(Rh_{2-y}Cr_yO_3)$/GaN photocatalyst because the $(Ga_{1-x}Zn_x)(N_{1-x}O_x)$ support has a larger surface area than the GaN support, leading to greater dispersion of the Rh^{3+}. When normalized by exposed surface Rh sites, the $(Rh_{2-y}Cr_yO_3)$/$(Ga_{1-x}Zn_x)(N_{1-x}O_x)$ is still 24× more active than the $(Rh_{2-y}Cr_yO_3)$/GaN due to the greater photon absorption efficiency of the $(Ga_{1-x}Zn_x)(N_{1-x}O_x)$ support than the GaN support.

The above surface/bulk characterization and photocatalytic studies allow for establishing surface/bulk structure−photoactivity relationships for photocatalytic splitting of water by GaN-based catalysts. The role of the GaN bulk lattice is to absorb photons to generate excited electron/hole pairs with UV excitation that can diffuse toward the surface of the photocatalyst to chemically react with water to form H_2 and O_2. The GaN bulk phase and its thin surface oxynitride film, however, are incapable of keeping photoexcited electron/hole pairs from recombining and performing photocatalytic splitting of water at the surface. The supported $(Rh_{2-y}Cr_yO_3)$ mixed oxide NPs are responsible for trapping and harnessing the photoexcited electrons at the surface of GaN to perform the water splitting reaction. The $(Rh_{2-y}Cr_yO_3)$ NPs were proposed to be the catalytic active site for H_2 production since the use of a sacrificial reagent (MeOH) for water splitting generated H_2 products only from supported $(Rh_{2-y}Cr_yO_3)$/GaN while GaN did not generate any H_2 products.[17] The GaN surface was proposed to be the catalytic active site for O_2 production since the use of a sacrificial reagent ($AgNO_3$) for water splitting generated O_2 products for GaN.[17] This suggests that the supported $(Rh_{2-y}Cr_yO_3)$ mixed oxide NPs harness the photoexcited electrons to evolve H_2 and the surface of the GaN support traps the photoexcited holes for reaction with water to evolve O_2 during photocatalytic splitting of water. These conclusions are consistent with the need for charge separation of the photoexcited electrons and holes at the surface of the supported $(Rh_{2-y}Cr_yO_3)$/GaN photocatalyst to perform photocatalysis. The presence of the GaO_x/GaO_xN_y oxynitride surface film on the GaN support may be critical for photocatalytic performance and also extends to the supported $(Rh_{2-y}Cr_yO_3)$/$(Ga_{1-x}Zn_x)(N_{1-x}O_x)$ photocatalyst system. A schematic model of the supported $(Rh_{2-y}Cr_yO_3)$/GaN photocatalyst system and its photocatalytic H_2O splitting pathways is shown in Figure 8.

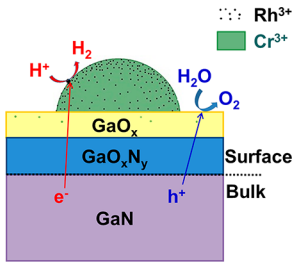

Figure 8. Schematic model of supported $(Rh_{2-y}Cr_yO_3)$/GaN photocatalyst system and its photocatalytic splitting of water.

EXPERIMENTAL METHODS

The bulk GaN was obtained from Mitsubishi Chemicals, which was prepared from elemental gallium. The GaN was mixed in an evaporating dish with the aqueous precursors of $Cr(NO_3)_3{\cdot}9H_2O$ (Wako Pure Chemicals, 99.9%) and $Na_3RhCl_6{\cdot}2H_2O$ (Kanto Chemicals, 97% as Rh) to yield a final composition of 1 wt % Rh and 1.5 wt % Cr. This suspension was then placed over a water bath and continuously stirred with a glass rod until complete evaporation. The powder was then collected and mildly calcined in air at 623 K for 1 h. The supported $(Rh_{2-y}Cr_yO_3)$/GaN photocatalyst was then washed with distilled water and dried overnight in an oven at 343 K.

The Raman spectra were obtained on a Lab Ram-HR Raman spectrometer. The UV−vis spectra were obtained on a Varian Cary 5E UV−vis spectrophotometer. A macro-Raman/photoluminescence system (Jobin Yvon Horiba, T6400) was used to obtain the photoluminescence spectra. The Scienta ESCA 300 spectrometer was used for HR-XPS analysis. The Qtac100 HS-LEIS Spectrometer (ION-TOF) was used to obtain HS-LEIS spectra.

ASSOCIATED CONTENT

Supporting Information

Detailed experimental methods. This material is available free of charge via the Internet at http://pubs.acs.org.

AUTHOR INFORMATION

Corresponding Author

*E-mail: iew0@lehigh.edu. Phone: (610)758-5149. Fax: (610) 758-6555.

Notes

The authors declare no competing financial interest.

dx.doi.org/10.1021/jz401884c | J. Phys. Chem. Lett. 2013, 4, 3719−3724

Present Address

[⊥](C.A.R.) Toyota Motor Engineering & Manufacturing North America, Inc., 1555 Woodridge Ave., Ann Arbor, Michigan 48105, United States.

■ ACKNOWLEDGMENTS

The authors gratefully acknowledge the financial support by the Department of Energy grant: DOE-FG02-93ER14350. A portion of this research was conducted at the Center for Nanophase Materials Sciences, which is sponsored at Oak Ridge National Laboratory by the Scientific User Facilities Division, Office of Basic Energy Sciences, U.S. Department of Energy in conjunction with User Project CNMS2008-075. The assistance of Dr. A. Miller at Lehigh University in obtaining and interpreting the HR-XPS and HS-LEIS data is also gratefully acknowledged.

■ REFERENCES

(1) Osterloh, F. E. Inorganic Materials as Catalysts for Photochemical Splitting of Water. *Chem. Mater.* **2008**, *20*, 35−54.

(2) Kudo, A.; Miseki, Y. Heterogeneous Photocatalyst Materials for Water Splitting. *Chem. Soc. Rev.* **2009**, *38*, 253−278.

(3) Chen, X.; Shen, S.; Guo, L.; Mao, S. S. Semiconductor-Based Photocatalytic Hydrogen Generation. *Chem. Rev.* **2010**, *110*, 6503−6570.

(4) Maeda, K.; Domen, K. New Non-Oxide Photocatalysts Designed for Overall Water Splitting Under Visible Light. *J. Phys. Chem. C* **2007**, *111*, 7851−7861.

(5) Sato, J.; Saito, N.; Yamada, Y.; Maeda, K.; Takata, T.; Kondo, J. N.; Hara, M.; Kobayashi, H.; Domen, K.; Inoue, Y. RuO_2-Loaded Beta-Ge_3N_4 as a Non-Oxide Photocatalyst for Overall Water Splitting. *J. Am. Chem. Soc.* **2005**, *127*, 4150−4151.

(6) Lee, Y.; Watanabe, T.; Takata, T.; Hara, M.; Yoshimura, M.; Domen, K. Effect of High-Pressure Ammonia Treatment on the Activity of Ge_3N_4 Photocatalyst for overall Water Splitting. *J. Phys. Chem. B* **2006**, *110*, 17563−17569.

(7) Maeda, K.; Saito, N.; Lu, D.; Inoue, Y.; Domen, K. Photocatalytic Properties of RuO_2-Loaded Beta-Ge_3N_4 for Overall Water Splitting. *J. Phys. Chem. C* **2007**, *111*, 4749−4755.

(8) Maeda, K.; Saito, N.; Inoue, Y.; Domen, K. Dependence of Activity and Stability of Germanium Nitride Powder for Photocatalytic Overall Water Splitting on Structural Properties. *Chem. Mater.* **2007**, *19*, 4092−4097.

(9) Maeda, K.; Teramura, K.; Lu, D.; Saito, N.; Inoue, Y.; Domen, K. Roles of Rh/Cr_2O_3 (Core/Shell) Nanoparticles Photodeposited on Visible-Light-Responsive $(Ga_{1-x}Zn_x)(N_{1-x}O_x)$ Solid Solutions in Photocatalytic Overall Water Splitting. *J. Phys. Chem. C* **2007**, *111*, 7554−7560.

(10) Maeda, K.; Teramura, K.; Lu, D.; Takata, T.; Saito, N.; Inoue, Y.; Domen, K. Characterization of Rh-Cr Mixed-Oxide Nanoparticles Dispersed on $(Ga_{1-x}Zn_x)(N_{1-x}O_x)$ as a Cocatalyst for Visible-Light-Driven Overall Water Splitting. *J. Phys. Chem. B* **2006**, *110*, 13753−13758.

(11) Maeda, K.; Teramura, K.; Lu, D.; Saito, N.; Inoue, Y.; Domen, K. Noble-Metal/Cr_2O_3 Core/Shell Nanoparticles as a Co-Catalyst for Photocatalytic Overall Water Splitting. *Angew. Chem., Int. Ed.* **2006**, *45*, 7806−7809.

(12) Maeda, K.; Teramura, K.; Domen, K. Effect of Post-Calcination on Photocatalytic Activity of $(Ga_{1-x}Zn_x)(N_{1-x}O_x)$ Solid Solution for Overall Water Splitting Under Visible Light. *J. Catal.* **2008**, *254*, 198−204.

(13) Maeda, K.; Teramura, K.; Saito, N.; Inoue, Y.; Domen, K. Improvement of Photocatalytic Activity of $(Ga_{1-x}Zn_x)(N_{1-x}O_x)$ Solid Solution for Overall Water Splitting by Co-Loading Cr and another Transition Metal. *J. Catal.* **2006**, *243*, 303−308.

(14) Lee, Y.; Terashima, H.; Shimodaira, Y.; Teramura, K.; Hara, M.; Kobayashi, H.; Domen, K.; Yashima, M. Zinc Germanium Oxynitride as a Photocatalyst for Overall Water Splitting Under Visible Light. *J. Phys. Chem. C* **2007**, *111*, 1042−1048.

(15) Arai, N.; Saito, N.; Nishiyama, H.; Inoue, Y.; Domen, K.; Sato, K. Overall Water Splitting by RuO_2-Dispersed Divalent-Ion-Doped GaN Photocatalysts with d^{10} Electronic Configuration. *Chem. Lett.* **2006**, *35*, 796−797.

(16) Arai, N.; Saito, N.; Nishiyama, H.; Domen, K.; Kobayashi, H.; Sato, K.; Inoue, Y. Effects of Divalent Metal Ion (Mg^{2+}, Zn^{2+} and Be^{2+}) Doping on Photocatalytic Activity of Ruthenium Oxide-Loaded Gallium Nitride for Water Splitting. *Catal. Today* **2007**, *129*, 407−413.

(17) Maeda, K.; Teramura, K.; Saito, N.; Inoue, Y.; Domen, K. Photocatalytic Overall Water Splitting on Gallium Nitride Powder. *Bull. Chem. Soc. Jpn.* **2007**, *80*, 1004−1010.

(18) Maeda, K.; Lu, D.; Domen, K. Direct Water Splitting into Hydrogen and Oxygen under Visible Light by Using Modified TaON Photocatalysts with d^0 Electronic Configuration. *Chem.—Eur. J.* **2013**, *19*, 4986−4991.

(19) Han, W.; Liu, Z.; Yu, H. Synthesis and Optical Properties of GaN/ZnO Solid Solution Nanocrystals. *Appl. Phys. Lett.* **2010**, *96*, 183112.

(20) Davydov, V.; Kitaev, Y.; Goncharuk, I.; Smirnov, A.; Graul, J.; Semchinova, O.; Uffmann, D.; Smirnov, M.; Mirgorodsky, A.; Evarestov, R. Phonon Dispersion and Raman Scattering in Hexagonal GaN and AlN. *Phys. Rev. B* **1998**, *58*, 12899−12907.

(21) Lee, E. L.; Wachs, I. E. Situ Spectroscopic Investigation of the Molecular and Electronic Structures of SiO_2 Supported Surface Metal Oxides. *J. Phys. Chem. C* **2007**, *111*, 14410−14425.

(22) Kim, D. S.; Tatibouet, J. M.; Wachs, I. E. Surface Structure and Reactivity of Chromium Trioxide/Silica Catalysts. *J. Catal.* **1992**, *136*, 209−21.

(23) Williams, C. T.; Takoudis, C. G.; Weaver, M. J. Methanol Oxidation on Rhodium as Probed by Surface-Enhanced Raman and Mass Spectroscopies: Adsorbate Stability, Reactivity, and Catalytic Relevance. *J. Phys. Chem. B* **1998**, *102*, 406−416.

(24) Brongersma, H.; Draxler, M.; Deridder, M.; Bauer, P. Surface Composition Analysis by Low-Energy Ion Scattering. *Surf. Sci. Rep.* **2007**, *62*, 63−109.

(25) Gilliland, G. D. Photoluminescence Spectroscopy of Crystalline Semiconductors. *Mater. Sci. and Eng.: R: Rep.* **1997**, *18*, 99−399.

(26) Anpo, M.; Kamat, P. V. *Environmentally Benign Photocatalysts: Applications of Titanium Oxide-based Materials*; Springer: New York, 2010.

(27) Hu, C.; Tsai, C.; Teng, H. Structure Characterization and Tuning of Perovskite-Like $NaTaO_3$ for Applications in Photoluminescence and Photocatalysis. *J. Am. Ceram. Soc.* **2009**, *92*, 460−466.

(28) Hu, C.; Lee, Y.; Teng, H. Efficient Water Splitting Over $Na_{1-x}K_xTaO_3$ Photocatalysts with Cubic Perovskite Structure. *J. Mater. Chem.* **2011**, *21*, 3824−3830.

(29) Singha, A.; Dhar, P.; Roy, A. A Nondestructive Tool for Nanomaterials: Raman and Photoluminescence Spectroscopy. *Am. J. Phys.* **2005**, *73*, 224−233.

(30) Maeda, K.; Teramura, K.; Saito, N.; Inoue, Y.; Domen, K. Improvement of Photocatalytic Activity of $(Ga_{1-x}Zn_x)(N_{1-x}O_x)$ Solid Solution for Overall Water Splitting by Co-Loading Cr and another Transition Metal. *J. Catal.* **2006**, *243*, 303−308.

(31) Maeda, K.; Teramura, K.; Domen, K. Development of Cocatalysts for Photocatalytic Overall Water Splitting on $(Ga_{1-x}Zn_x)$-$(N_{1-x}O_x)$ Solid Solution. *Catal. Surv. Asia* **2007**, *11*, 145−157.

(32) Maeda, K.; Teramura, K.; Takata, T.; Hara, M.; Saito, N.; Toda, K.; Inoue, Y.; Kobayashi, H.; Domen, K. Overall Water Splitting on $(Ga_{1-x}Zn_x)(N_{1-x}O_x)$ Solid Solution Photocatalyst: Relationship between Physical Properties and Photocatalytic Activity. *J. Phys. Chem. B* **2005**, *109*, 20504−20510.